Supporting Information

Synthesis of 4H/*fcc* noble multimetallic nanoribbons for electrocatalytic hydrogen evolution reaction

Zhanxi Fan,[1†] Zhimin Luo,[1†] Xiao Huang,[2] Bing Li,[3] Ye Chen,[1] Jie Wang,[1] Yanling Hu,[1] and Hua Zhang*[1]

[1]Center for Programmable Materials, School of Materials Science and Engineering, Nanyang Technological University, 50 Nanyang Avenue, Singapore 639798, Singapore

[2]Key Laboratory of Flexible Electronics (KLOFE) & Institute of Advanced Materials (IAM), Jiangsu National Synergistic Innovation Center for Advanced Materials (SICAM), Nanjing Tech University (NanjingTech), 30 South Puzhu Road, Nanjing 211816, China

[3]Institute of Materials Research and Engineering, Agency for Science, Technology and Research, 2 Fusionopolis Way, Innovis #08-03, Singapore 138634, Singapore

[†]These authors made equal contributions to this work.

[*]Corresponding author.

Fax: (+65) 67909081

E-mail: hzhang@ntu.edu.sg

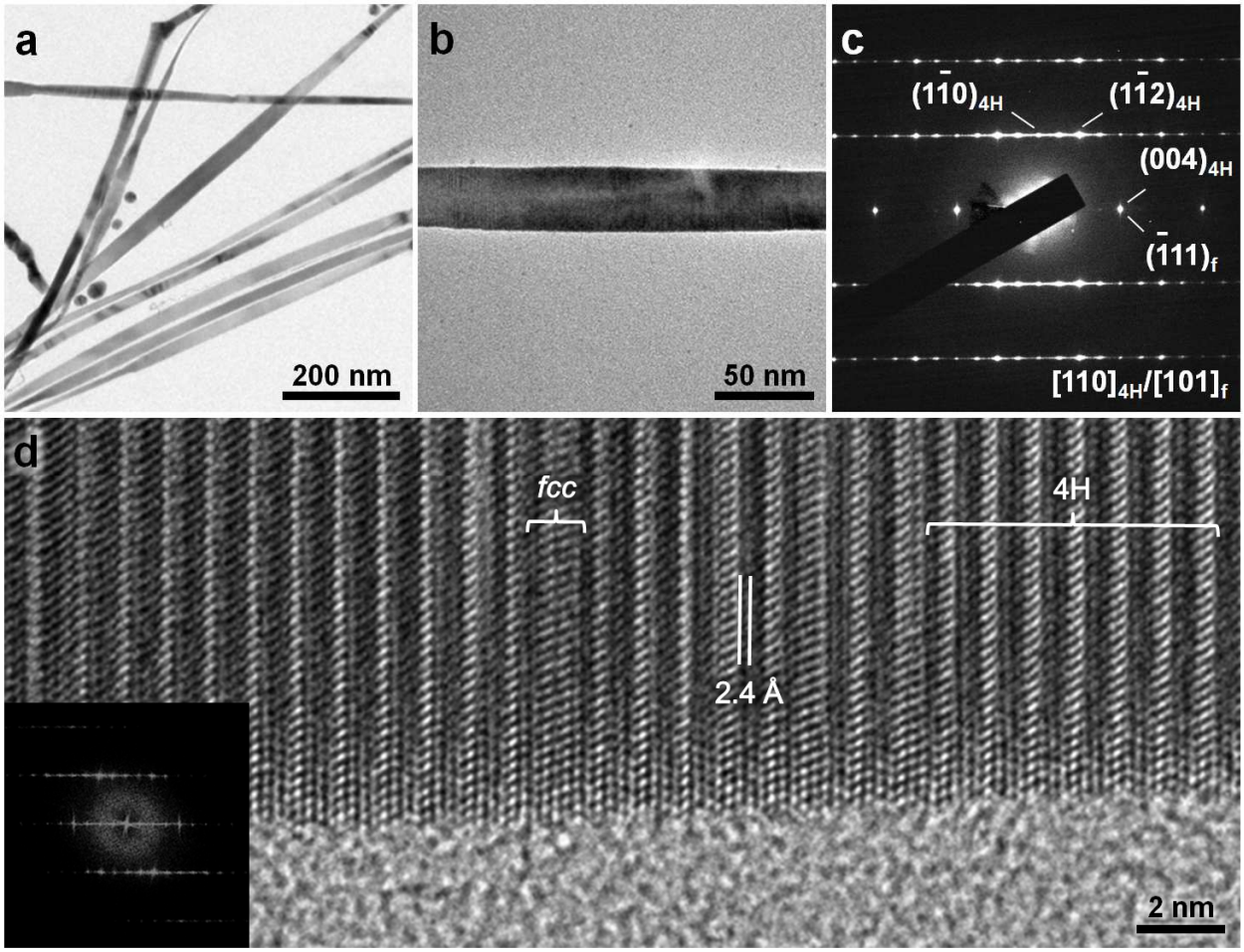

Figure S1. (a) Low-magnification TEM image of the as-prepared 4H/*fcc* Au@Ag NRBs. (b) High-magnification TEM image of a typical 4H/*fcc* Au@Ag NRB. (c) The corresponding SAED pattern of a typical 4H/*fcc* Au@Ag NRB taken along the $[110]_{4H}/[101]_f$ zone axes. (d) A typical HRTEM image of the 4H/*fcc* Au@Ag NRB. Inset: The corresponding FFT pattern of the HRTEM image shown in (d).

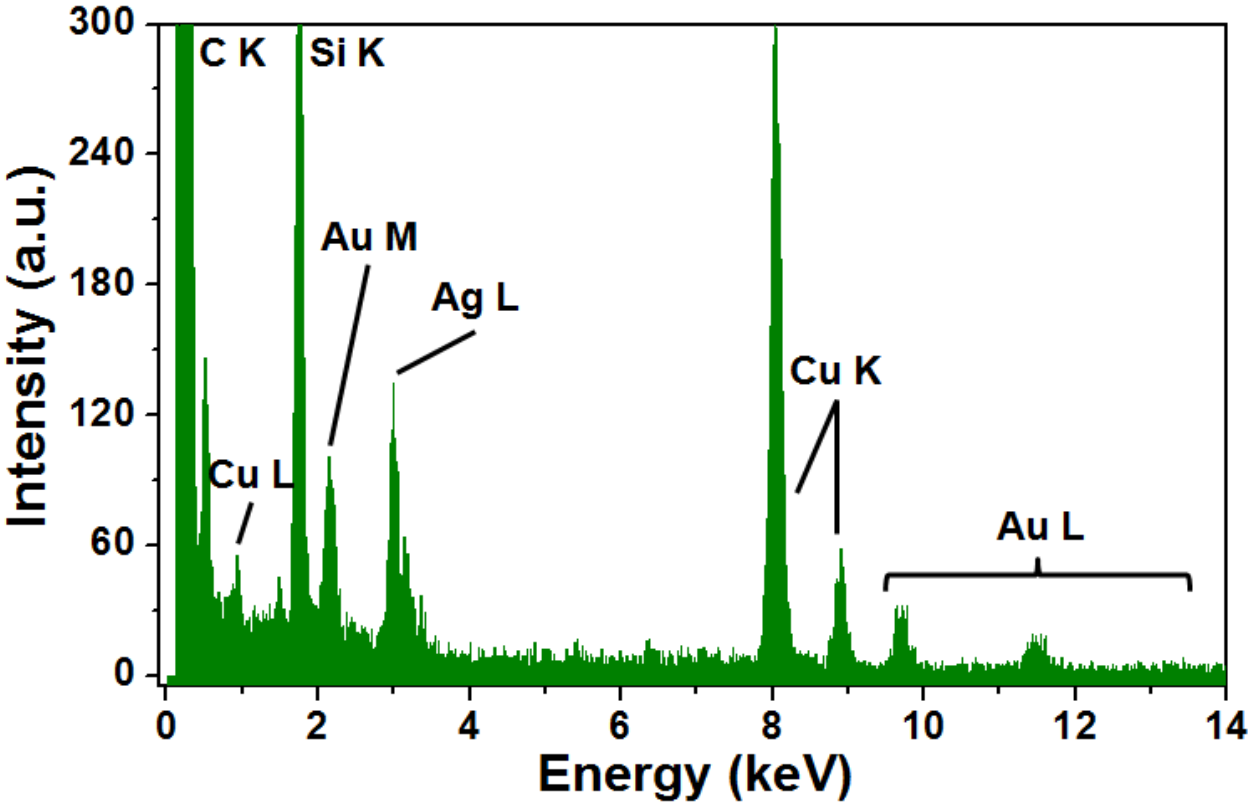

Figure S2. A typical STEM-EDS spectrum of 4H/*fcc* Au@Ag NRBs, giving average Au/Ag atomic ratio of about 1.00/2.60.

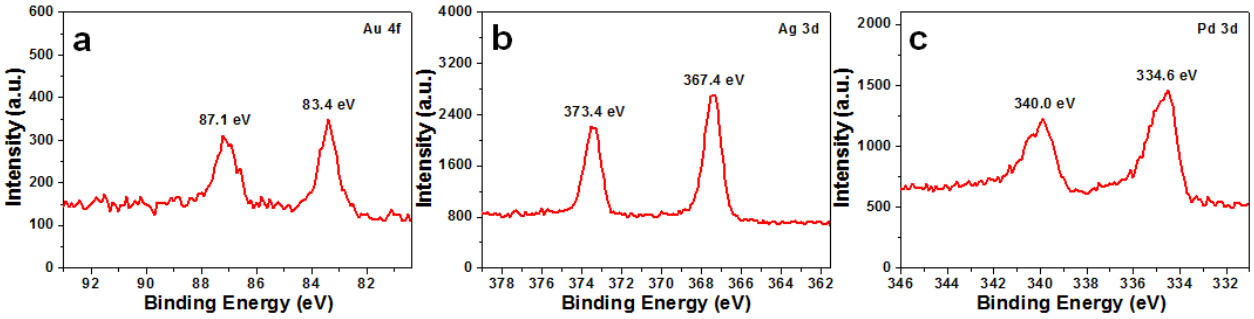

Figure S3. XPS spectra of 4H/*fcc* Au@PdAg NRBs showing the core level peaks of (a) Au4f, (b) Ag3d, and (c) Pd3d.

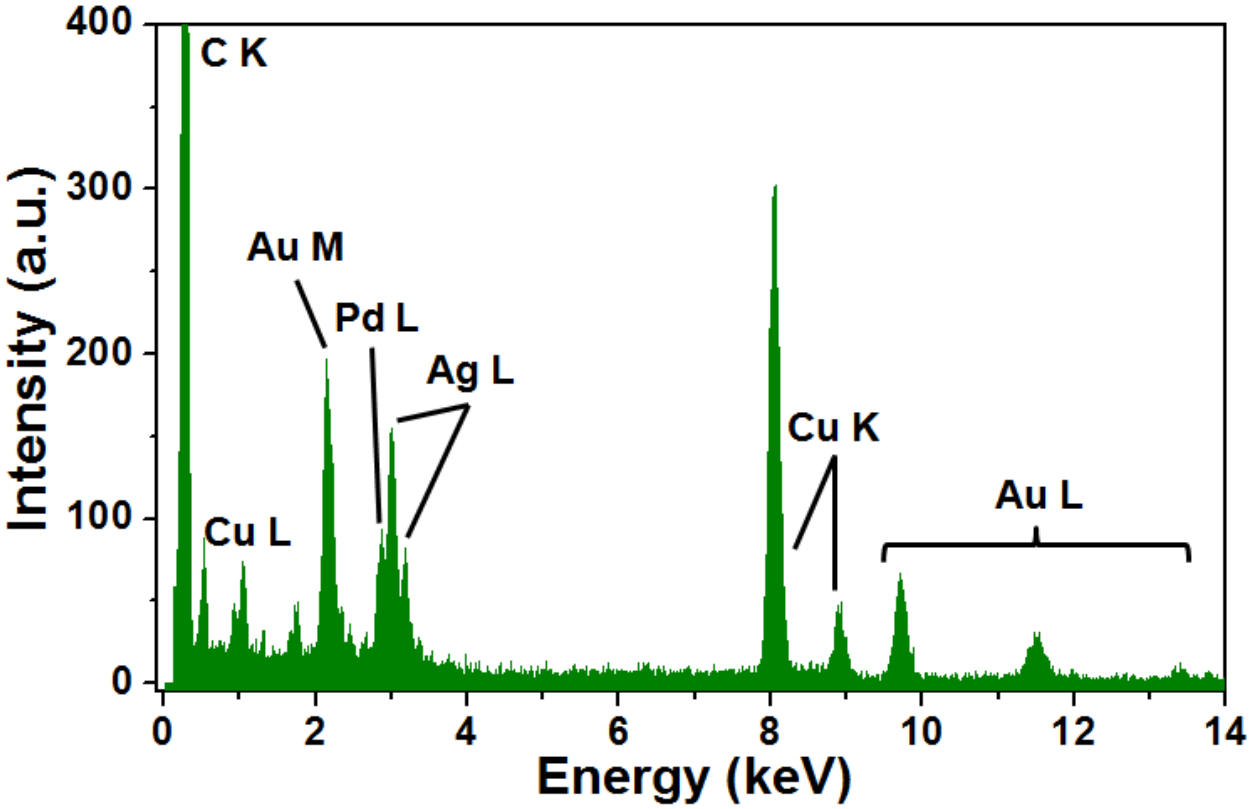

Figure S4. A typical STEM-EDS spectrum of 4H/*fcc* Au@PdAg NRBs, giving average Au/Ag/Pd atomic ratio of about 1.00/1.94/1.06.

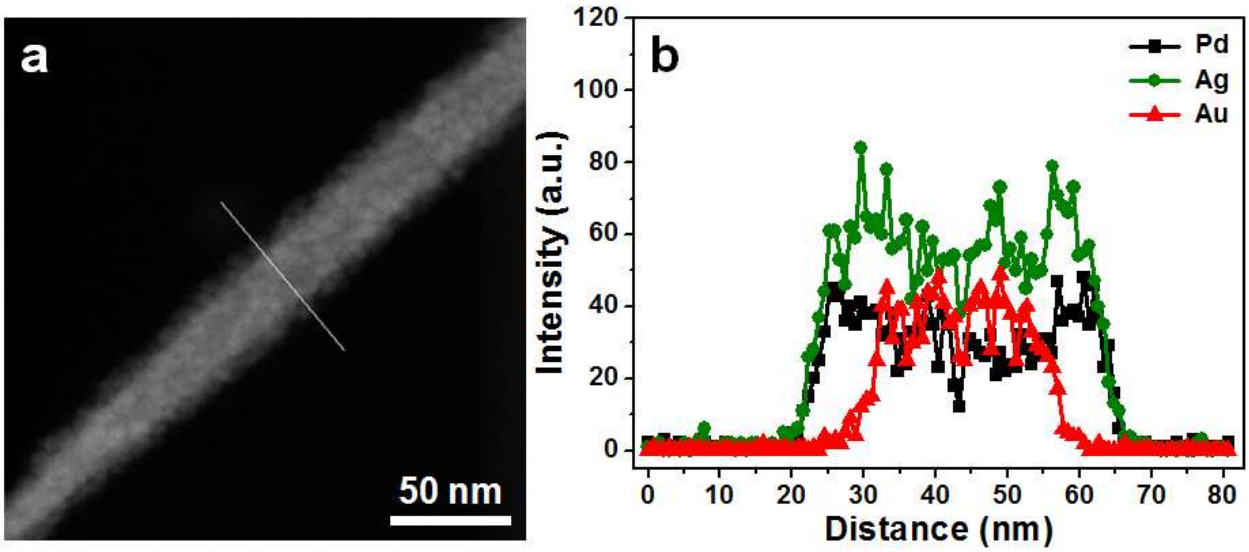

Figure S5. (a) HAADF-STEM image and (b) the corresponding STEM-EDS line scanning profile of a typical 4H/*fcc* Au@PdAg NRB.

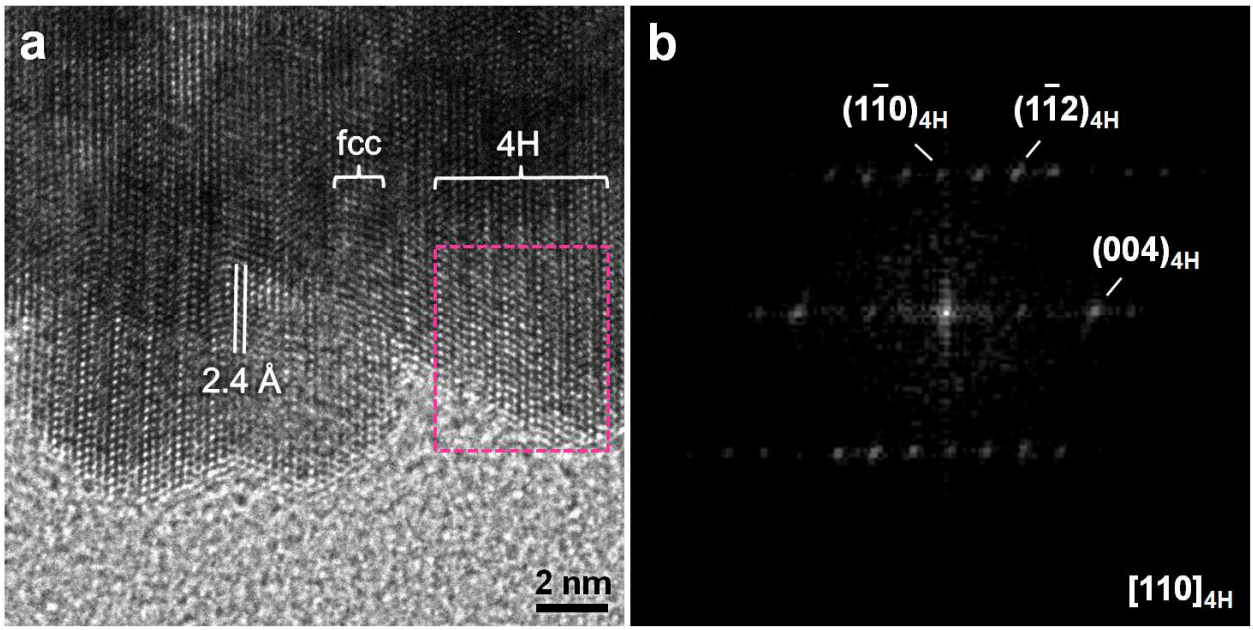

Figure S6. (a) HRTEM image of a typical 4H/*fcc* Au@PdAg NRB (same image in Fig. 2f). (b) The corresponding FFT pattern of the selected area, i.e. the dashed rectangle, in (a). The FFT pattern clearly reveals the formation of PdAg alloy shell with 4H hexagonal phase.[1]

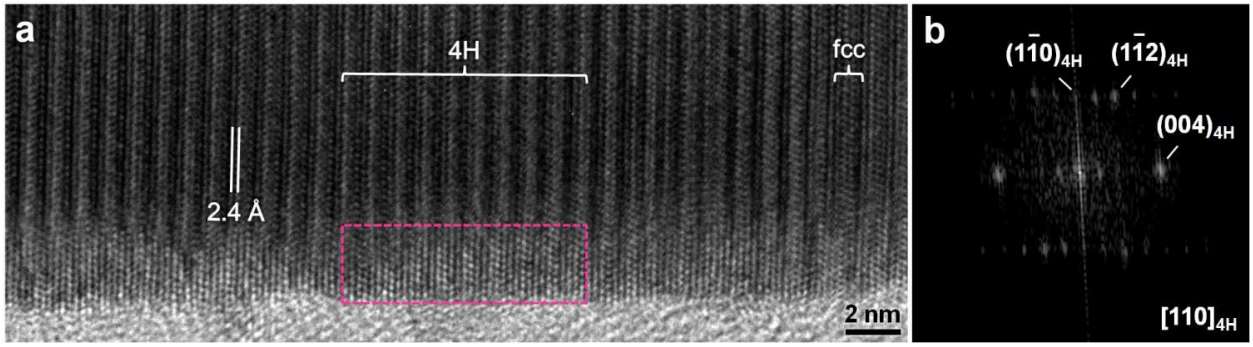

Figure S7. (a) HRTEM image of a typical 4H/*fcc* Au@PtAg NRB (same image in Fig. 3e). (b) The corresponding FFT pattern of the dashed rectangle in (a). The FFT pattern clearly reveals the formation of PtAg alloy shell with 4H hexagonal phase.[1]

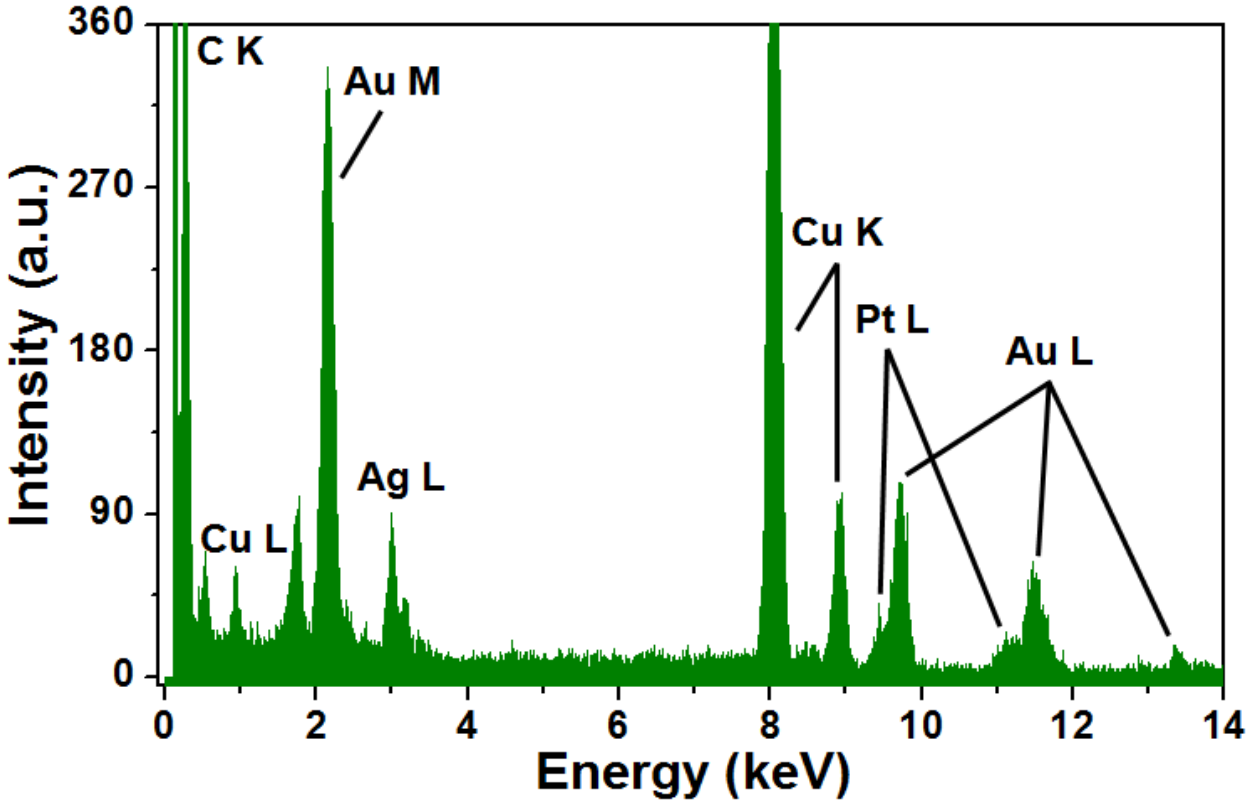

Figure S8. A typical STEM-EDS spectrum of 4H/*fcc* Au@PtAg NRBs, giving average Au/Ag/Pt atomic ratio of about 1.00/0.58/0.23.

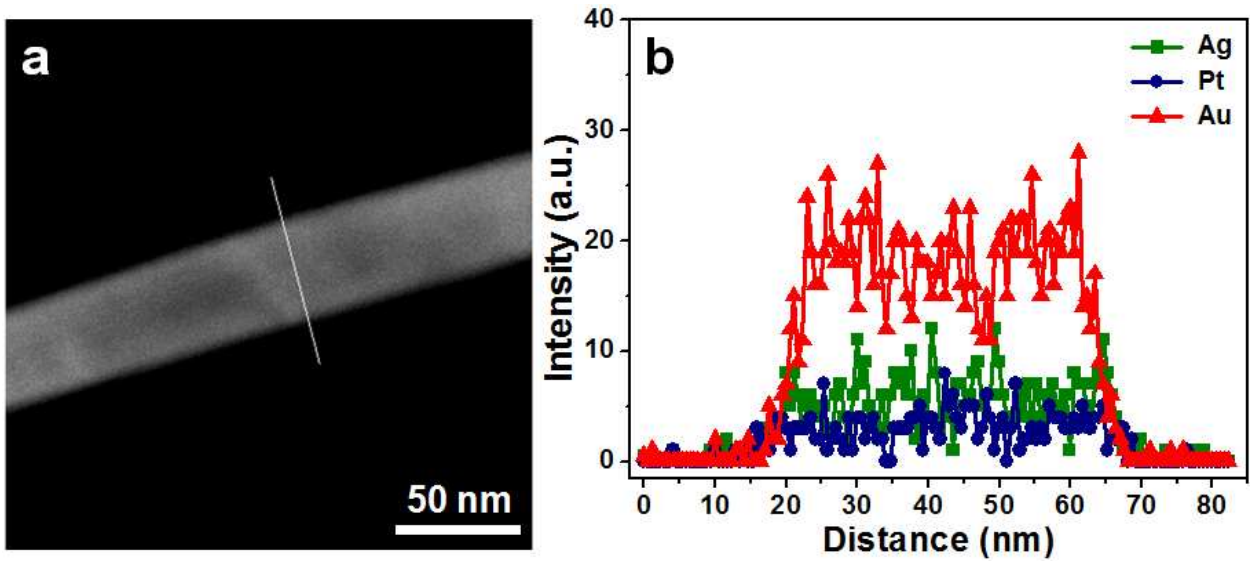

Figure S9. (a) HAADF-STEM image and (b) the corresponding STEM-EDS line scanning profile of a typical 4H/*fcc* Au@PtAg NRB.

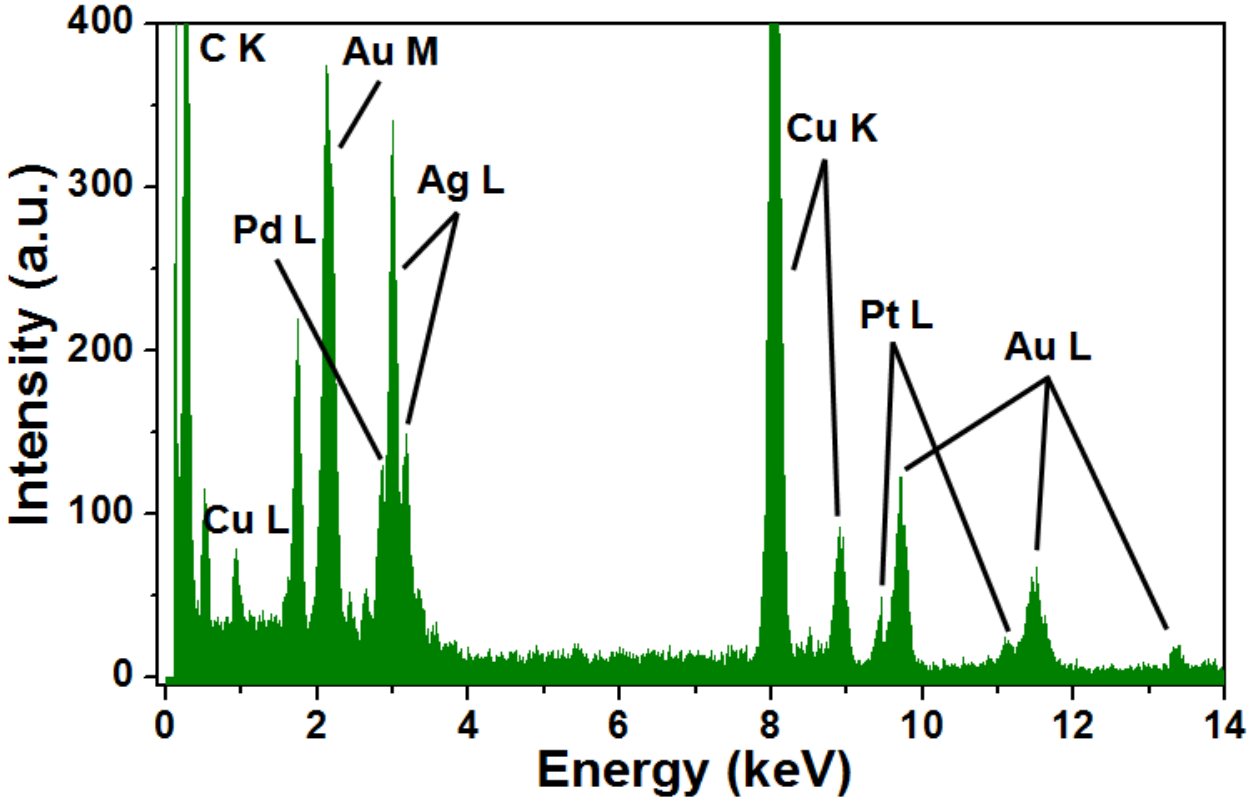

Figure S10. A typical STEM-EDS spectrum of 4H/*fcc* Au@PtPdAg NRBs, giving average Au/Ag/Pd/Pt atomic ratio of about 1.00/1.85/0.84/0.29.

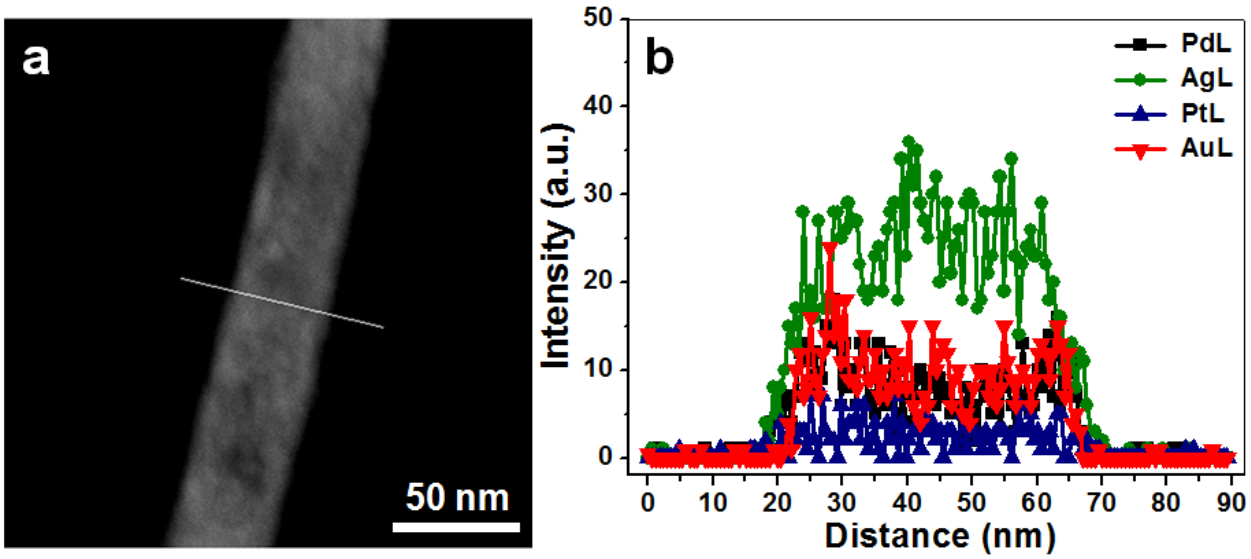

Figure S11. (a) HAADF-STEM image and (b) the corresponding STEM-EDS line scanning profile of a typical 4H/*fcc* Au@PtPdAg NRB.

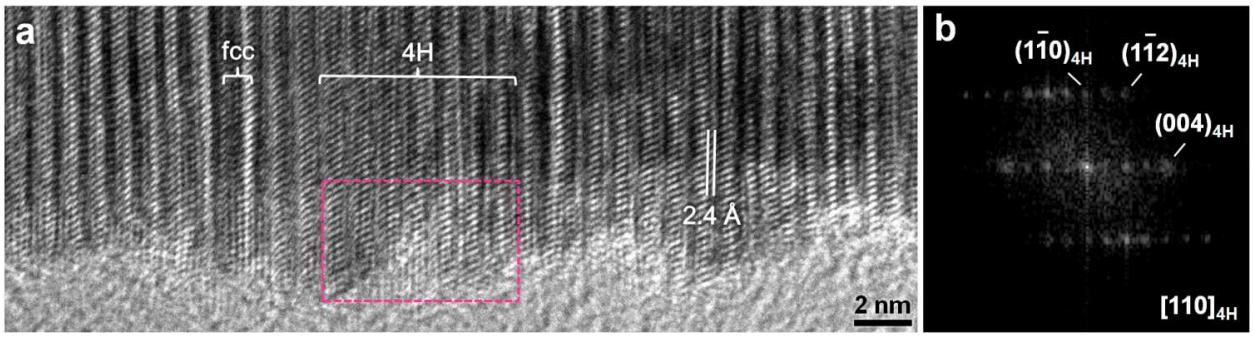

Figure S12. (a) HRTEM image of a typical 4H/*fcc* Au@PtPdAg NRB (same image in Fig. 4e). (b) The corresponding FFT pattern of the dashed rectangle in (a). The FFT pattern clearly reveals the formation of PtPdAg alloy shell with 4H hexagonal phase.[1]

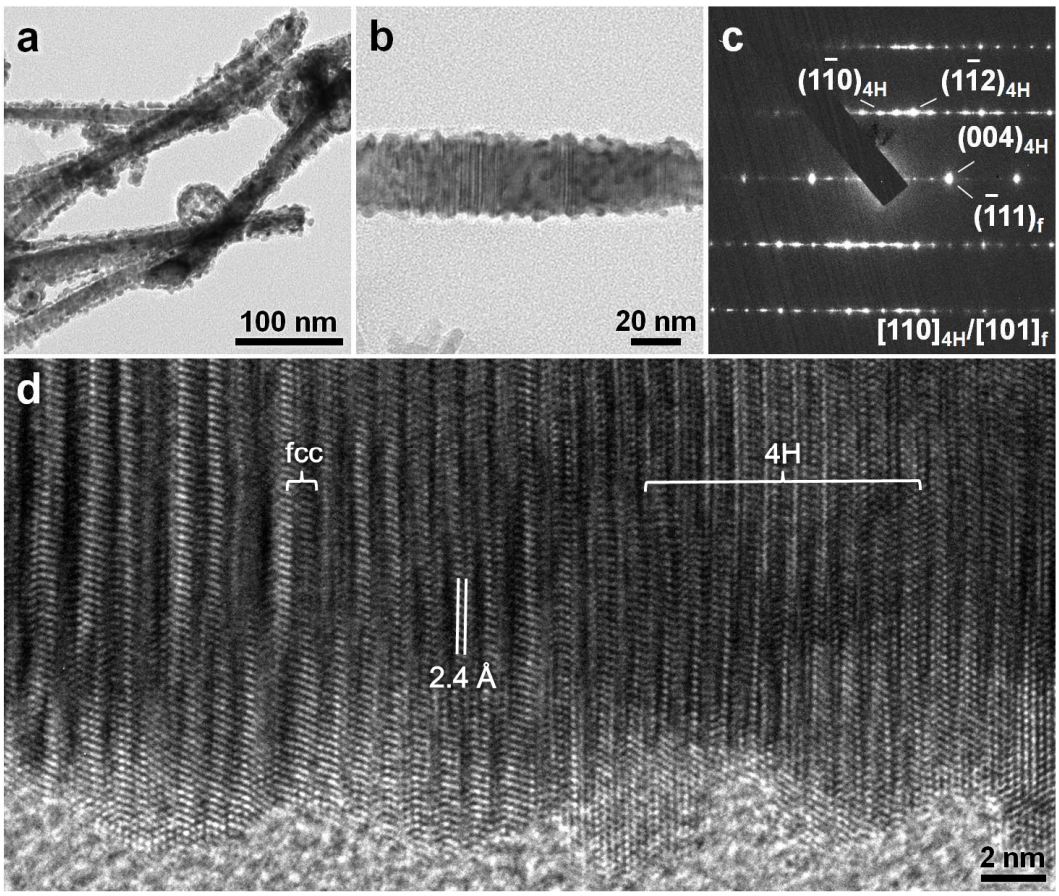

Figure S13. (a) Low-magnification TEM image of 4H/*fcc* Au@PdAg NRBs after 10000 potential cycles. (b) High-magnification TEM image and (c) the corresponding SAED pattern taken along the $[110]_{4H}/[101]_f$ zone axes of a typical 4H/*fcc* Au@PdAg NRB after 10000 potential cycles. (d) A typical HRTEM image of the 4H/*fcc* Au@PdAg NRB after 10000 potential cycles.

The TEM images in (a) and (b) show that the rough surface morphology of Au@PdAg NRBs was well preserved after 10000 potential cycles. Moreover, the 4H/*fcc* structure of Au@PdAg NRBs was also well maintained after 10000 potential cycles, as confirmed by the SAED pattern in (c) and HRTEM image in (d). The aforementioned results indicate that both the shape and crystal structure of 4H/*fcc* Au@PdAg NRBs are quite stable toward the electrocatatlytic HER.

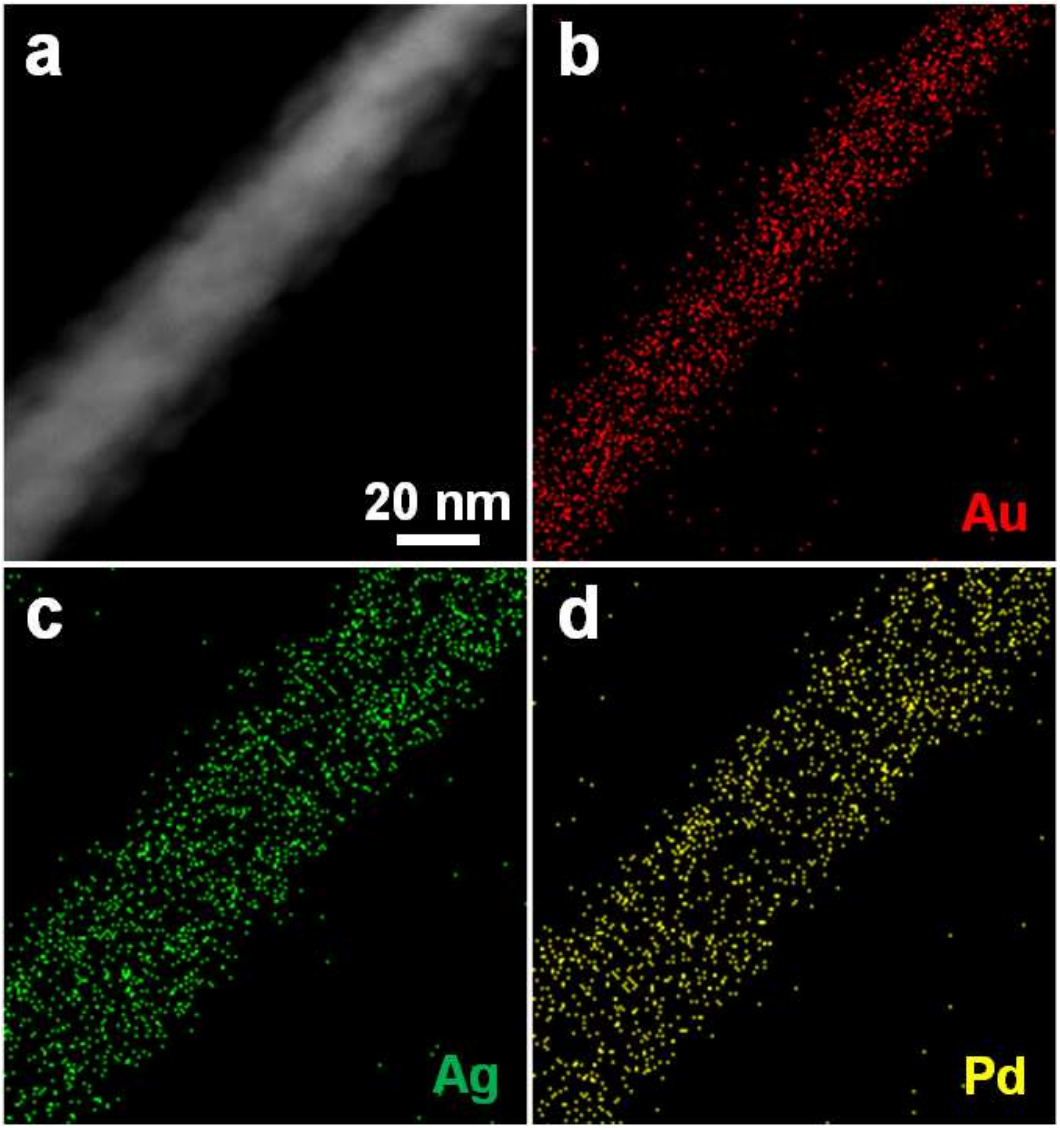

Figure S14. (a) HAADF-STEM image and (b−d) the corresponding STEM-EDS elemental mappings of a representative 4H/*fcc* Au@PdAg NRB after 10000 potential cycles.

The HAADF-STEM image in (a) clearly reveals that the core-shell architecture, i.e. bright core (Au) and dark shell (PdAg), of the Au@PdAg NRB was well preserved after the 10000 potential cycles. Furthermore, the STEM-EDS elemental mappings in (b–c) identify the homogeneous distribution of Au, Ag and Pd in the Au@PdAg NRB after the 10000 potential cycles.

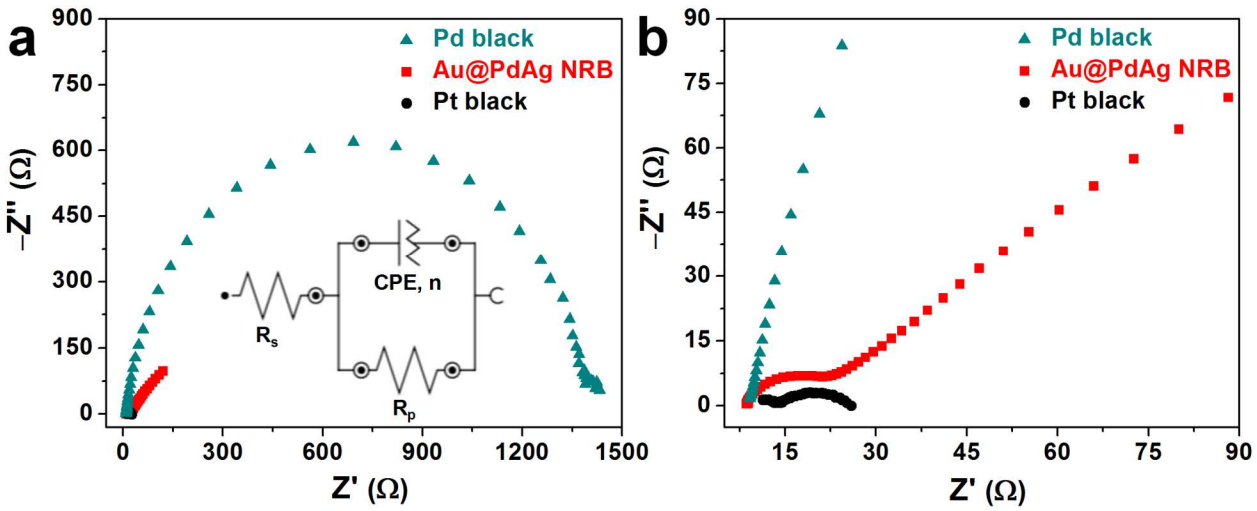

Figure S15. (a) Electrochemical impedance spectroscopy (EIS) data for the electrode modified with Pd black, Au@PdAg NRBs and Pt black. The inset is an equivalent circuit for electrochemical circle fitting, where R_s, R_p, CPE, and n represent the uncompensated resistance, the charge transfer resistance, the argument of constant phase element, and the exponent of the constant phase element, respectively. (b) The magnified EIS data in a. The calculated charge transfer resistances of Pd black, Au@PdAg NRBs and Pt black are 1410.2 Ω, 16.2 Ω, and 11.5 Ω, respectively.

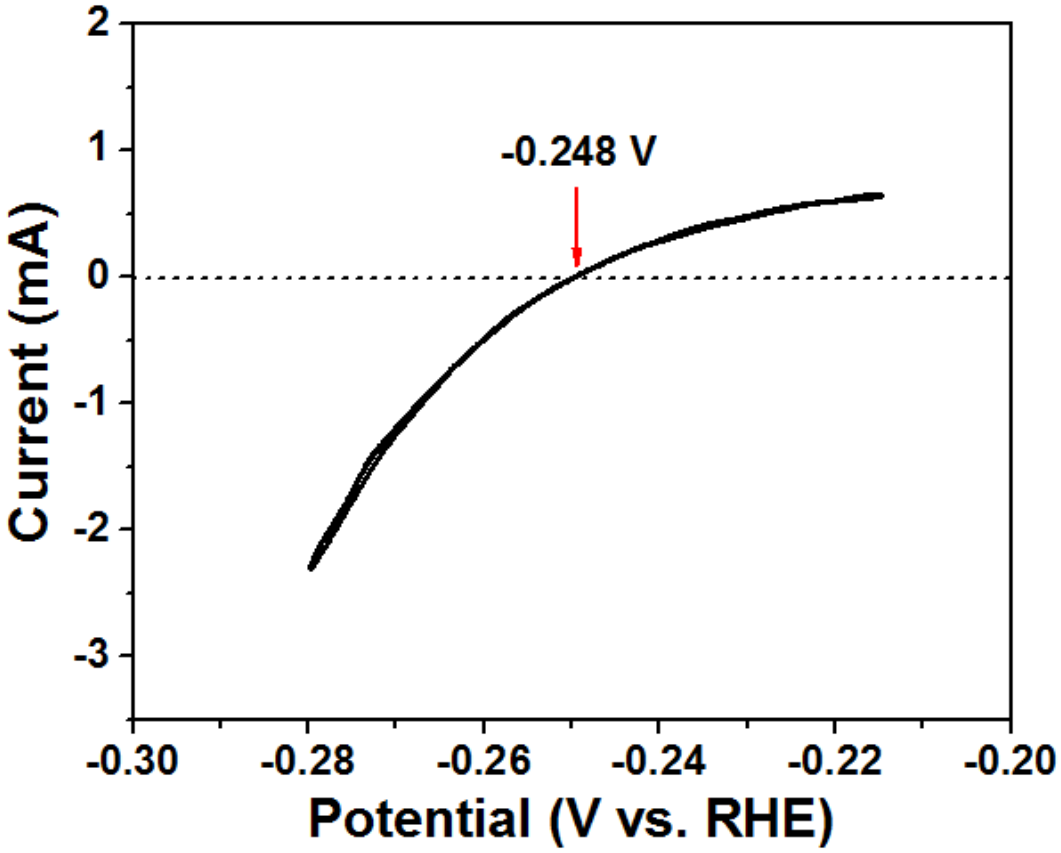

Figure S16. Current–potential curve for the calibration of Ag/AgCl electrode with respect to RHE in the highly pure H_2-saturated 0.5 M H_2SO_4 by using a Pt wire as the working electrode.

Reference

(1) Fan, Z. X.; Bosman, M.; Huang, X.; Huang, D.; Yu, Y.; Ong, K. P.; Akimov, Y. A.; Wu, L.; Li, B.; Wu, J.; Huang, Y.; Liu, Q.; Png, C. E.; Gan, C. L.; Yang, P. D.; Zhang, H. *Nat. Commun.* **2015**, *6*, 7684.